

Electronic Supplementary Information

Ultrafine Rh nanocrystals grown onto boron and nitrogen codoped carbon support with a horn-shaped structure for highly efficient methanol oxidation

Xiangjie Guo,^a Jie Xiong,^a Qi Wang,^a Jian Zhang,^b Haiyan He,^a Huajie Huang^{*a}

^aCollege of Mechanics and Materials, Hohai University, Nanjing 210098, China

^bNew Energy Technology Engineering Lab of Jiangsu Province, College of Science, Nanjing University of Posts & Telecommunications (NUPT), Nanjing 210023, China

*E-mail: huanghuajie@hhu.edu.cn

Supplementary Results:

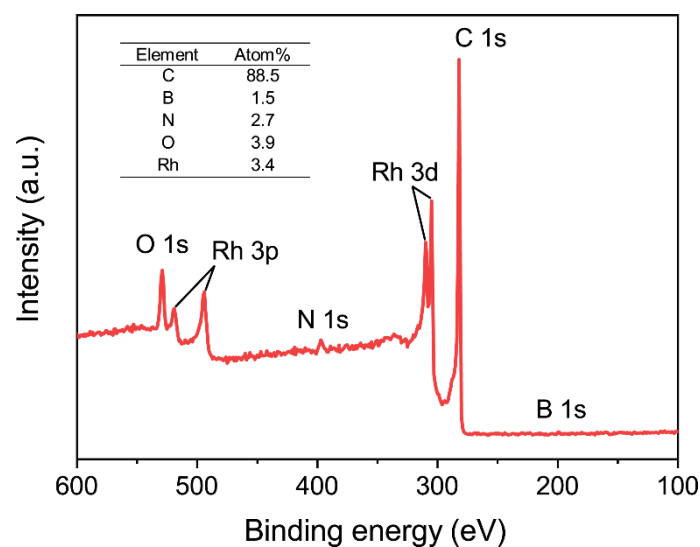


Fig. S1 The XPS survey spectrum and elemental quantitative analysis of the Rh/BNCNH hybrid.

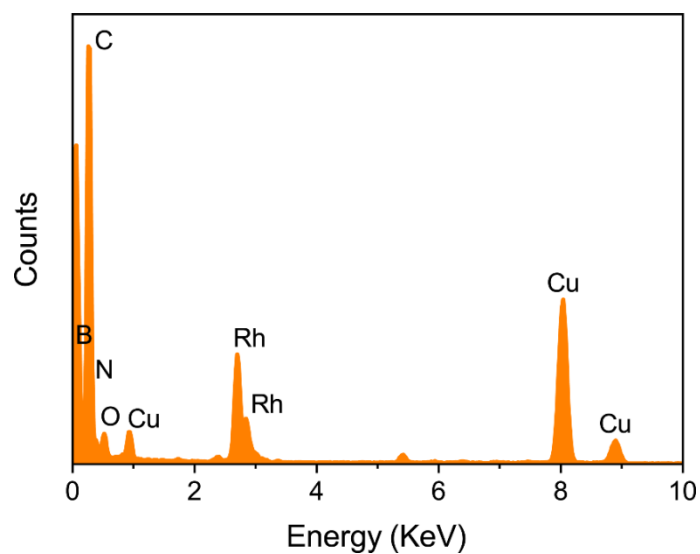


Fig. S2 EDX spectrum of Rh(20%)/BNCNH catalyst verifies the presence of B, C, N, O, and Rh components in the hybrid.

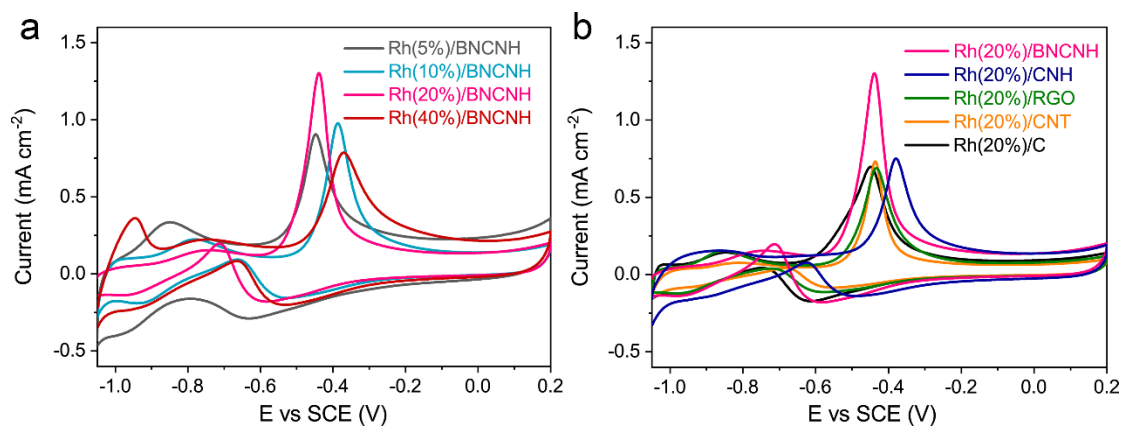


Fig. S3 The ECSA-normalized CV curves of (a) the Rh/BNCNH with different Rh dosages, and (b) Rh(20%)/CNH, Rh(20%)/RGO, Rh(20%)/CNT, and Rh(20%)/C catalysts in 1 M KOH with 1 M CH₃OH solution at 50 mV s⁻¹.

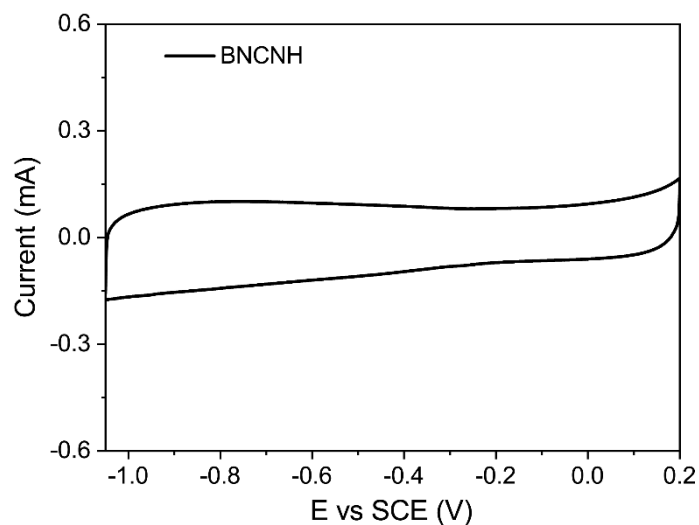


Fig. S4 The CV curve of the BNCNH catalyst in 1 M KOH with 1 M CH₃OH solution at 50 mV s⁻¹.

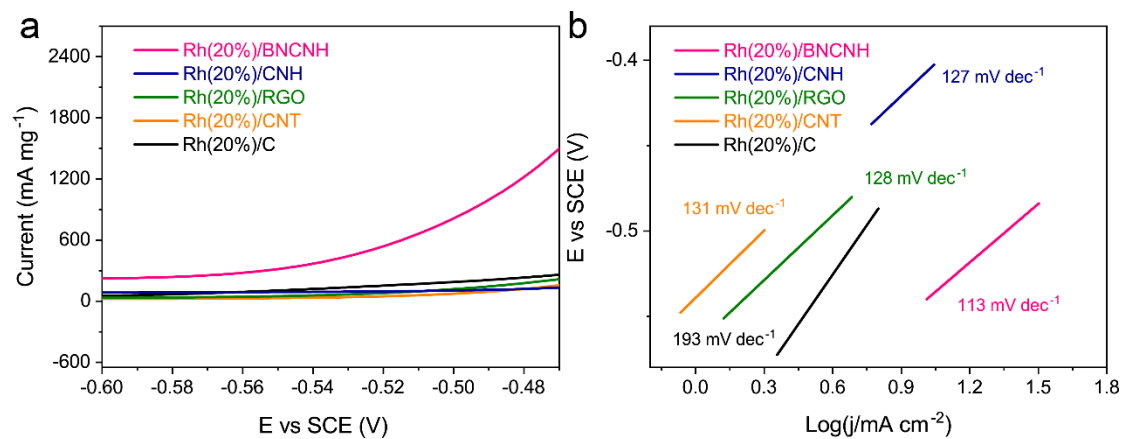


Fig. S5 (a) Linear sweep voltammeters of Rh(20%)/BNCNH, Rh(20%)/CNH, Rh(20%)/RGO, Rh(20%)/CNT, and Rh(20%)/C electrodes in 1 M KOH with 1 M CH₃OH solution at 50 mV s⁻¹. (b) Tafel plots of the Rh(20%)/BNCNH, Rh(20%)/CNH, Rh(20%)/RGO, Rh(20%)/CNT, and Rh(20%)/C electrodes.

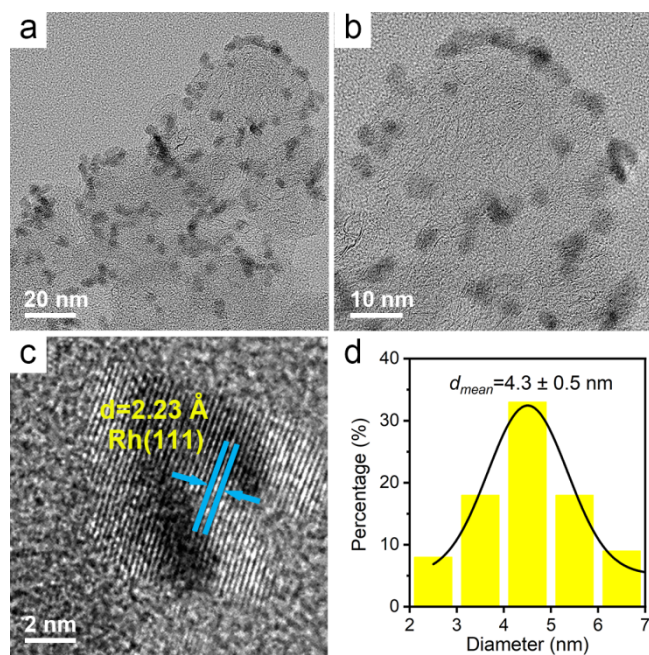


Fig. S6 Typical (a-b) TEM, (c) HRTEM images, and (d) Rh particle size distribution of the Rh/BNCNH catalyst after the stability test.

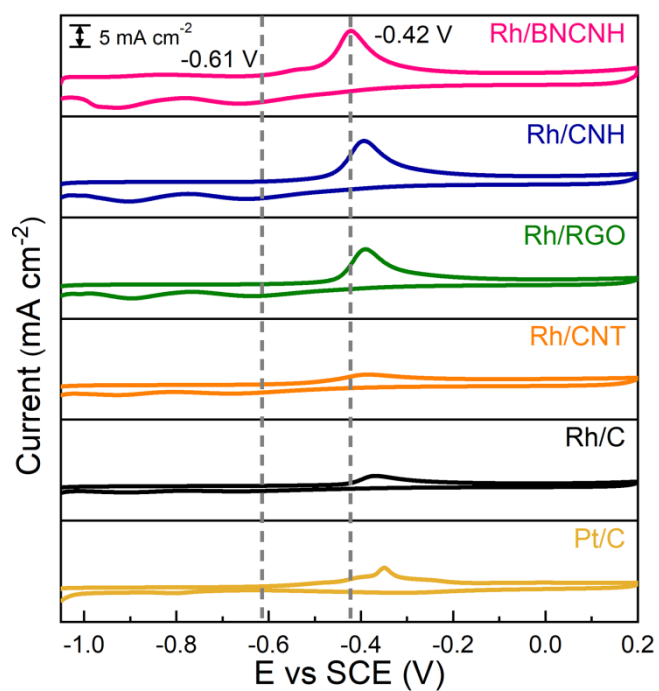


Fig. S7 CO stripping voltammograms for the Rh/BNCNH, Rh/CNH, Rh/RGO, Rh/CNT, Rh/C, and Pt/C electrodes in 1 M KOH solution at 50 mV s⁻¹.

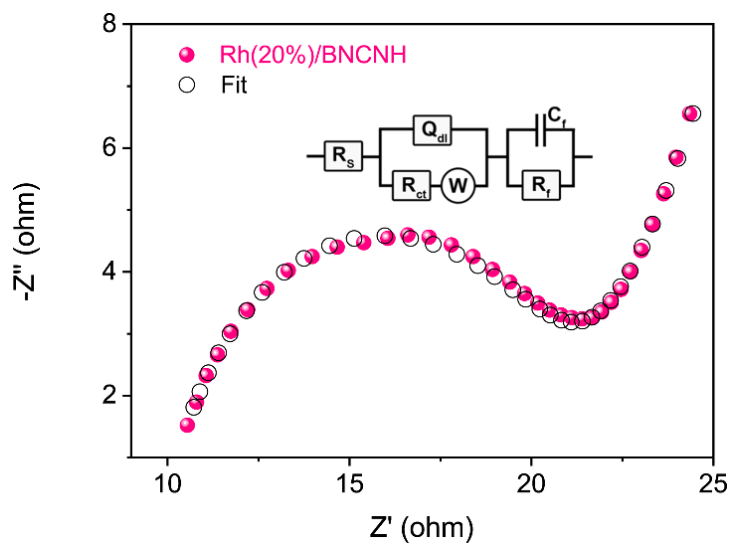


Fig. S8 AC impedance spectrum of the Rh(20%)/BNCNH electrode and the corresponding fitting curve. The inset is the equivalent circuit used to fit the spectrum.

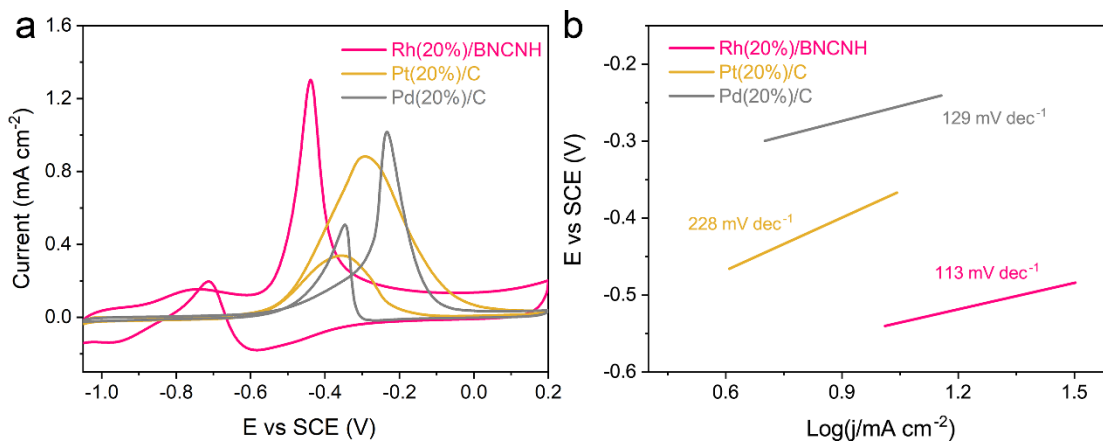


Fig. S9 (a) The ECSA-normalized CV curves of Rh(20%)/BNCNH, Pt(20%)/C, and Pd(20%)/C catalysts in 1 M KOH with 1 M CH₃OH solution at 50 mV s⁻¹. (b) Tafel plots of the Rh(20%)/BNCNH, Pt(20%)/C, and Pd(20%)/C electrodes.

Table S1 Electrochemical behaviors on different catalysts in DMFC condition

Electrode	ECSA ($\text{m}^2 \text{g}^{-1}$)	Mass activity (mA mg^{-1})	Specific activity (mA cm^{-2})
Rh(5%)/BNCNH	42.5	270.3	0.64
Rh(10%)/BNCNH	132.3	1280.6	0.97
Rh(20%)/BNCNH	182.4	2350.5	1.29
Rh(40%)/BNCNH	93.6	750.2	0.80
Rh(20%)/CNH	68.3	575.4	0.84
Rh(20%)/RGO	53.7	369.7	0.69
Rh(20%)/CNT	46.4	339.3	0.73
Rh(20%)/C	42.8	290.1	0.68
Pt(20%)/C	59.5	525.0	0.88
Pd(20%)/C	65.2	663.0	1.01

Table S2 Comparison of the methanol oxidation behaviors on the Rh(20%)/BNCNH catalyst with various state-of-the-art Rh-based electrocatalysts.

Electrode	ECSA ($\text{m}^2 \text{g}^{-1}$)	Mass activity (mA mg^{-1})	Electrolyte	Ref.
Rh(20%)/BNCNH	182.4	2350.5	1 mol L ⁻¹ KOH+1 mol L ⁻¹ CH ₃ OH	This work
Rh/3D graphene	79.6	498.9	1 mol L ⁻¹ KOH+1 mol L ⁻¹ CH ₃ OH	[23]
Rh sheet/graphene	48.7	264.0	1 mol L ⁻¹ KOH+1 mol L ⁻¹ CH ₃ OH	[42]
Rh sheets	73.1	333.0	1 mol L ⁻¹ KOH+0.5 mol L ⁻¹ CH ₃ OH	[43]
Rh nanowires	144.2	722.0	1 mol L ⁻¹ KOH+1 mol L ⁻¹ CH ₃ OH	[44]
Rh nanotubes	60.9	325.0	1 mol L ⁻¹ KOH+1 mol L ⁻¹ CH ₃ OH	[40]
Rh dendrites	43.4	255.6	1 mol L ⁻¹ KOH+1 mol L ⁻¹ CH ₃ OH	[45]

Table S3. The charge transfer resistances of different catalysts.

Electrode	R_{ct}	
	Value (ohm)	Error (%)
Rh(20%)/BNCNH	10.2	2.2
Rh(20%)/CNH	8.4	3.1
Rh(20%)/RGO	13.6	2.9
Rh(20%)/CNT	16.3	4.7
Rh(20%)/C	7438.5	4.1